

A comparative analysis of 5-azacytidine and zebularine induced DNA demethylation

Patrick T. Griffin, Chad E. Niederhuth, and Robert J. Schmitz

Department of Genetics, University of Georgia, Athens, GA, 30602, USA

Corresponding author:

Robert J. Schmitz
University of Georgia
120 East Green Street, Athens, GA 30602
Telephone: (706) 542-1887
Fax: (706) 542-3910
E-mail: schmitz@uga.edu

Abstract

The non-methylable cytosine analogs, 5-azacytidine and zebularine, are widely used to inhibit DNA methyltransferase activity and reduce genomic DNA methylation. In this study, whole-genome bisulfite sequencing is used to construct maps of DNA methylation with single base pair resolution in *Arabidopsis thaliana* seedlings treated with each demethylating agent. We find that both inhibitor treatments result in nearly indistinguishable patterns of genome-wide DNA methylation and that 5-azacytidine had a slightly greater demethylating effect across the genome at higher concentrations. Transcriptome analyses revealed a substantial number of up-regulated genes, with an overrepresentation of transposable element genes, in particular CACTA-like elements. This demonstrates that chemical demethylating agents have a disproportionately large effect on loci that are otherwise silenced by DNA methylation.

Introduction

Cytosine DNA methylation, the covalent addition of a methyl group to the 5' carbon of a cytosine nucleotide, is required for viability in plants and mammals that possess this base modification. Its presence or absence is known to influence gene expression (Finnegan et al. 1993), heterochromatin status (Mathieu et al. 2007), and genomic integrity through transposon silencing (Saze and Kakutani 2007; Johannes et al. 2009; Reinders et al. 2009). In mammals, DNA methylation covers most of the genome with the exception of certain unmethylated CG dinucleotides "CpG islands" (Kafri et al. 1992), and aberrant DNA methylation is associated with cancer in humans (Ohm et al. 2007; Widschwendter et al. 2007; Gal-Yam et al. 2008). In plants, DNA methylation is distributed differently than in mammals and is found enriched at pericentromeric regions and at lower levels on chromosome ends (Zhang et al. 2006; Zilberman et al. 2007; Cokus et al. 2008; Lister et al. 2008; Niederhuth and Schmitz 2014). Because DNA methylation in flowering plants is meiotically inherited and changes in DNA methylation states can affect morphological variation, it is thought of as a latent reservoir of phenotypic diversity (Ji et al. 2015). Consequently, its manipulation has been pursued in recent years to discover potentially beneficial new traits, particularly in crop species.

The diversity of DNA methylation patterns in plants is attributed in part to the variety of DNA methyltransferase enzymes that establish and maintain it. Methylated CG sites (mCG), regardless of their location in the genome, are faithfully propagated and maintained by DNA METHYLTRANSFERASE 1 (MET1) (Finnegan et al. 1996). CHG methylation (mCHG) is most commonly found in transposons and repeat elements, and it is maintained by a feed forward loop that requires the activity of the DNA methyltransferase CHROMOMETHYLASE 3 (CMT3) and the histone methyltransferase KRYPTONITE (KYP) (Jackson et al. 2002; Cao et al. 2003; Du et al. 2012). Curiously, CMT3 also appears to be involved in the establishment of gene body DNA methylation (gbM), as it was recently discovered that species that have lost CMT3 have no gbM (Bewick et al. 2016). CHH methylation (mCHH) is dependent on either CMT2 or DOMAINS REARRANGED METHYLTRANSFERASE 2 (DRM2). CMT2 largely acts in deep heterochromatin regions of the genomes as well as within the bodies of large transposons (Zemach et al. 2013). In contrast, DRM2, as part of the RNA-directed DNA Methylation (RdDM) pathway, methylates mostly at the edges of repeats and transposons in euchromatin (Law and Jacobsen 2010).

The development of whole-genome bisulfite sequencing (WGBS) has advanced the understanding of DNA methylation in plant genomes (Cokus et al. 2008; Lister et al. 2008). A comprehensive analysis of WGBS on *Arabidopsis thaliana* mutants defective for DNA methylation helped describe the specific roles of RdDM-associated enzymes and siRNA-independent DNA methylation enzymes, while also establishing the interplay between the two pathways (Stroud et al. 2013). These and other studies continue to provide a valuable resource to

plant researchers interested in the mechanistic underpinnings of how DNA methylation is established and maintained in plant genomes.

The chemical inhibition of DNA methyltransferases has been utilized as a transient alternative to study the effect of DNA methylation loss in plants (Pecinka and Liu 2014). Two of the most widely used chemical demethylating agents, 5-azacytidine (AZA) and zebularine (ZEB), act as non-methylable cytosine analogs; incorporating into the DNA double helix in the place of cytosine with each cycle of DNA replication (Pecinka and Liu 2014). Previous studies have shown that AZA covalently binds to DNA methyltransferases, forming nucleoprotein adducts, which depletes the number of active DNA methyltransferase enzymes in the cell (Jones and Taylor 1980; Creusot et al. 1982; Christman et al. 1983; Santi et al. 1984). ZEB, a more stable alternative to AZA, inhibits DNA methylation in a similar manner, although it is not thought to form an irreversible bond with DNA methyltransferases (Champion et al. 2010). Although AZA and ZEB have been widely used in plants, a genome-wide, comprehensive analysis of either chemical on DNA methylomes has been missing.

In this study, we use WGBS to compare the genome-wide effects of AZA or ZEB treatment on *A. thaliana* seedlings. Although each demethylating agent seems to have an indiscriminate, concentration-dependent effect genome-wide, AZA may be more effective at higher concentrations. mCG was found to be proportionally less impacted by AZA in comparison with mCHH in both the pericentromeres and chromosome arms. RNA-seq was performed to identify potential effects of chemical demethylation on gene expression. Transposable element genes were by far the most highly upregulated class, in particular CACTA-like elements. Genes with high amounts of methylation in all contexts were more highly upregulated than those categorized as gene body-methylated genes. The results of this study help to further clarify the effect of non-methylable cytosine analogs on DNA methylation genome-wide and will provide a guide for future application of these tools.

Methods

I. Seed sterilization, plate preparation, and chemical treatments

Agarose gel (Ameresco) with added half-strength Linsmaier and Skoog nutrients (Caisson Laboratories, Inc) was prepared and autoclaved. 5-azacytidine (Sigma) and zebularine (APExBIO) were dissolved in dimethyl-sulfoxide (DMSO) and water, respectively, before being added to the liquefied cooling agar at final concentrations of 25 μ M, 50 μ M and 100 μ M. Columbia-0 (Col-0) background *A. thaliana* seeds were subjected to an ethanol-based seed sterilization and approximately 30 seeds plated per treatment. As a control, seeds were plated on agar containing DMSO with no chemical demethylating agent (AZA mock-treated control), or agar containing neither DMSO nor chemical demethylating agent (untreated control). After a two-day stratification period at 4°C, the seeds were transferred to room temperature and allowed to grow for 8 days under constant light.

II. DNA extraction and Whole-Genome Bisulfite Sequencing

A. thaliana seedlings from each agar plate were pooled and DNA was extracted using the DNeasy Plant Mini Kit (QIAGEN). MethylC-seq libraries were prepared as previously outlined (Urich et al. 2015). Briefly, sonicated DNA (sheared to ≈ 200 -400 bp) was selected with Ser-Mag Speed Beads (Thermo Scientific) and then subjected to end-repair, A-tailing, and adaptor ligation. The DNA was then treated with sodium bisulfite from the EZ DNA Methylation Gold Kit (Zymo Research) and the bisulfite converted DNA was PCR-amplified for 10 cycles. After cleanup of the PCR product, the DNA libraries were sequenced using the Illumina Next-Seq 500 at the Georgia Genomics Facility. One sample from each treatment group and control group was deeply sequenced, with average coverage of 23.0 to 28.1 (**Table S1**). Downstream analysis was carried out on FASTQ files that were mapped to the TAIR10 reference genome after being trimmed for adaptors and preprocessed to remove low quality reads using Methylpy (Schultz et al. 2015b; Schultz et al. 2015a). A second replicate of control samples and seedlings treated with 100 μ M of AZA or ZEB were lightly sequenced (**Table S2**) and run through the web tool *FASTmC*, a tool for genome-wide estimation of DNA methylation levels (Bewick et al. 2015).

Genome-wide methylation levels from deeply-sequenced samples were calculated using weighted methylation (Schultz et al. 2012). BedTools (Quinlan and Hall 2010) was used to make windows of consistent sizes across the genome and extract methylation data for genomic features. Custom scripts in Python were used to calculate methylation levels from windows produced by Bedtools. Custom scripts in R were used to rearrange data sets and visually represent the data. Further, the linear model function in R, *lm()*, was used to determine the association between demethylating agent concentration and DNA methylation levels (e.g. *lm(weighted methylation ~ concentration)*) (**Table S3**).

A. thaliana genes were classified as gene-body methylated (gbM), mCHG-enriched, or mCHH-enriched using a previously defined list (Niederhuth et al. 2016). Briefly, genes were tested for enrichment of mCG, mCHG, and mCHH sites in coding sequences against a background methylation rate using a binomial test (Takuno and Gaut 2012). Genes enriched for mCG, but not mCHG or mCHH, were classified as gbM genes. Genes enriched for mCHG, but not mCHH were classified as mCHG-enriched genes. These genes can also contain mCG, which is often found alongside mCHG. mCHH-enriched genes were those genes enriched for mCHH, but could also contain mCG and mCHG (Soppe et al. 2000; Niederhuth et al. 2016).

III. RNA-seq

Col-0 seeds were treated with 100 μ M of 5-azacytidine alongside DMSO mock-treated controls as before. RNA was extracted using TRIzol (Thermo Scientific) and RNA libraries were made using the TruSeq Stranded mRNA Library Prep Kit (Illumina). Three replicates of AZA-treated seedlings and four

replicates of mock-treated seedling were then sequenced using the Illumina Next-Seq 500 instrument at the Georgia Genomics Facility. Reads were mapped to the TAIR10 *A. thaliana* reference genome using the default settings of Tophat 2 version 2.0.14 (Kim et al. 2013). Cuffdiff software version 2.2.1 with default settings was used to calculate expression levels and identify differentially expressed genes (Trapnell et al. 2013). To eliminate infinite expression differences, 0.1 was added to every expression value, and the \log_2 -fold-changes between treated and untreated samples were calculated. P-values were corrected for multiple testing using Benjamini-Hochberg False Discovery Rate (q value). Genes were considered differentially expressed with a $q < 0.05$ and a \log_2 -fold-change greater than 2.0 or less than -2.0.

In assessing the enrichment of upregulated methylation-categorized (e.g. gbM, mCHG genes, etc) and transposable element genes, each subgroup was subjected to a Fischer's Exact Test via the `fisher.test()` function in R. Methylation-categorized gene categories were tested as a subset of all genes, whereas transposable element gene categories were tested against all transposable element genes.

Results

To assess the effect of AZA and ZEB, a sample of each treatment was deeply sequenced using WGBS and the genome-wide methylation level for all cytosines in each context of DNA methylation were plotted (**Figure 1A**, **Table S2**). A concentration-dependent decrease in DNA methylation was observed in both AZA- and ZEB-treated DNA. The relationship between DNA methylation and chemical concentration was highly correlated (all p values < 0.05) for DNA treated with either AZA ($r^2 = 0.99$) and ZEB ($r^2 = 0.88$) for all methylated cytosines, and for CG (AZA $r^2 = 0.99$; ZEB $r^2 = 0.93$) and CHG methylation (AZA $r^2 = 0.96$; ZEB $r^2 = 0.99$) specifically (**Table S3**). This observation suggests that at 100 μM , neither the effect of AZA nor ZEB on CG or CHG methylation is saturated. CHH methylation did not substantially decrease between the 50 μM and 100 μM -treated samples for either AZA- or ZEB-treated seedlings, suggesting some amount of saturation. Consequently, the relationship between inhibitor concentration and methylation loss was less highly correlated (AZA $r^2 = 0.65$; ZEB $r^2 = 0.61$). A second replicate of seedlings treated with 100 μM AZA and ZEB using low coverage sequencing combined with *FASTmC* analysis confirmed the genome-wide loss of DNA methylation (see Methods) (**Table S3**). Although this technique is less sensitive, it also shows a concentration dependent decrease in both AZA and ZEB up until 100 μM .

To compare the genome-wide demethylating potential of each chemical, the methylation level of the treated samples relative to the control was plotted (**Figure 1B**). For consistency, each sample was compared to the untreated control (no DMSO added). The effect of the chemicals is similar but not identical, with either AZA or ZEB having a slightly greater effect at lower concentrations (25 μM and 50 μM). At a concentration of 100 μM , however, AZA had an 8.0% and

10.2% larger demethylating effect on mCG and mCHG, respectively. This was unexpected since the seedlings were treated for 10 days without replenishing the chemicals, and AZA has a far shorter degradation half-life than ZEB at room temperature (Champion et al. 2010). Both chemicals were found to reduce the distribution of methylation levels at highly methylated CG sites (**Figure 1C**), shifting the percentage of methylated CG dinucleotides that are completely methylated from 32.8% in the untreated control to 3.9% in 100 μ M AZA-treated seedlings and 8.5% in 100 μ M ZEB-treated seedlings.

To examine how AZA and ZEB affect methylation across chromosomes, the methylation level was calculated for 50 kb bins across chromosome 1 (**Figure 2A**). DNA methylation was reduced across chromosome 1 in a concentration-dependent manner, most notably for CG and CHG in the pericentromeric region. To illustrate the magnitude of demethylation along the genome, the methylation level of AZA and ZEB-treated DNA relative to that in the control DNA was plotted for each window across chromosome 1 (**Figure 2B**) and all chromosomes (**Figure S1**). CG methylation, maintained at higher levels than mCHG and mCHH across the genome (Zhang et al. 2006; Zilberman et al. 2007; Cokus et al. 2008; Lister et al. 2008), is consistently affected across the entire chromosome, whereas the loss of CHG and CHH methylation is greatest in the pericentromere. To eliminate bias from unmethylated regions and compare the demethylating effect in the pericentromere and chromosome arms, the genome was further broken up into 100 bp windows, and the 100 μ M AZA-treated and mock-treated control methylation levels were plotted pairwise for both regions on chromosome 1 (**Figure 2C-D**). Viewed this way, it becomes clear that AZA treatment affects highly methylated regions in both the pericentromere and chromosome arms equally, resulting in similar levels of demethylation. Given the evidence that RNA-independent DNA methyltransferases are the primary mediators of DNA methylation in the pericentromere, whereas gene body DNA methylation and RdDM activity are primarily found in the chromosome arms (Stroud et al. 2013; Zemach et al. 2013), this result suggests that chemical demethylating agents act without bias on the different pathways. Of note, windows with high CHH methylation (>25% methylation levels) tended to lose 50% to 75% of it in the AZA-treated sample (**Figure 2C**), whereas, CG methylation was less impacted, hovering between 25% and 50% loss (**Figure 2D**). Similar results were found in analyzing the 100 μ M ZEB-treated sample against the untreated control (**Figure S3**).

The associated effect of DNA methylation on genes depends upon the methylation profile within the genes. Genes that are only methylated in the CG context are known as gene body methylated (gbM) and these genes are often expressed and moderate levels (Tran et al. 2005; Zhang et al. 2006; Zilberman et al. 2007). This is in contrast to genes that are methylated in all contexts as they are associated with lower gene expression or silencing (Law and Jacobsen 2010). Genes were previously classified into one of four classes based on their methylation profile (Niederhuth et al. 2016). Coding sequences of gbM genes are

methyated in the CG context only. CHG-enriched (mCHG) genes contain significant numbers of methylated CHG, but not CHH sites, whereas CHH-enriched (mCHH) genes contain significant numbers of methylated CHH sites and are typically methylated in all sequence contexts. To investigate the effect of AZA and ZEB on these different gene classes, average methylation was plotted across the gene bodies and 1500 base pairs up- and downstream. In gbM genes, DNA methylation at CGs is reduced in a concentration-dependent manner for both AZA and ZEB (**Figure S2A**). Similarly, mCHH genes and transposons show a concentration-dependent loss of DNA methylation in all contexts (**Figure S2C-D**). Comparing the 100 μ M AZA and ZEB samples reveals that DNA methylation in all sequence features is more reduced by AZA, except for the CHH context in mCHH genes (**Figure 3A-C**). Similarly, the difference in methylation level of AZA- and ZEB-treated seedlings across transposons (**Figure 3C**) is less drastic for CHH methylation. This could suggest that at 100 μ M, the effect of each drug is saturated.

Methylation in all three contexts is often indicative of RdDM (Law and Jacobsen 2010) and can reduce gene expression of reporter genes (Hohn et al. 1996; Dieguez et al. 1997). Furthermore, previous studies have demonstrated that both AZA and ZEB reactivate transcription of silenced genetic elements in plants (Chang and Pikaard 2005; Baubec et al. 2014). To investigate the impact of DNA methylation inhibitors on the different methylation-based gene categories, we performed RNA-seq on seedlings treated with 100 μ M of AZA. Out of all genes, 1060 were significantly upregulated and 263 were significantly downregulated in comparison to the mock-treated control (**Table S4**). Of these, 516 were protein-coding genes and 503 were classified as transposable element (TE) genes, a disproportionate amount when compared to the totality of genes annotated in the *A. thaliana* genome (**Figure 3D**). Of protein-coding genes, mCHH genes were found to be significantly enriched in upregulated genes based on a Fischer's Exact Test (p value $< 2.2 \times 10^{-16}$), whereas mCHG and gbM genes were not significantly enriched (**Figure 3E, Table S4**). To further investigate effects on TE genes, differential expression of individual TE families was examined (**Figure 3F**). Out of all TE genes, 12.9% were upregulated. Copia-like elements were the least affected, with only 23 out of 491 genes (4.68%) upregulated. In contrast, the most highly upregulated category of TE genes was CACTA-like elements (29.8%) and they were the only category of TE genes that was significantly enriched when compared to all other TE genes (p value = 7.04×10^{-12} , Fisher's Exact Test).

Having investigated methylation-based gene classes and TE genes, we next examined specific genes, *FLOWERING WAGENINGEN* (*FWA*) and *SUPPRESSOR of *drm1 drm2* and *cmt3** (*SDC*), that do not fit into our methylation-based categories and nonetheless are known to be transcriptionally silenced by DNA methylation (Soppe et al. 2000; Kinoshita et al. 2007; Henderson and Jacobsen 2008). Although methylation was not completely lost, methylation levels were reduced, without bias to the sequence context (**Figure**

4A-D). This is similar to what was observed genome-wide. Whether this is the result of a complete loss of DNA methylation in some cell types, which leads to reactivation of transcription, or if there is partial loss of DNA methylation in all cell types, remains to be investigated. *FWA* and *SDC* were among the top 10% of AZA-upregulated genes, with mRNA expression increased 5.4-fold and 6.9-fold respectively (**Table S5**). These well-studied genes, where the association of gene expression and epigenetic silencing has been established, along with the increased expression of many mCHH genes, provides further evidence that perturbation of DNA methylation by inhibitors predictably reactivates certain genetic elements.

Discussion

In this study, we have examined the genome-wide effects of the chemical demethylating agents 5-azacytidine and zebularine. Known to have analogous modes of action (Pecinka and Liu 2014), our analysis demonstrates that both chemicals have similar effects, as DNA methylation is depleted across the entire genome in all sequence contexts. In previous studies, it had been estimated that at 40 μ M, ZEB is a more effective demethylating agent than AZA (Baubec et al. 2009). Our estimates of relative methylation loss show that AZA may have a larger effect than ZEB at higher concentrations, whereas at lower concentrations, the difference is less clear. The differences in these results between labs may be explained by differences in growth medium composition, treatments of the plant material, growth conditions and duration of treatment. It could also suggest that certain loci are more susceptible at lower concentrations than others with regards to transcriptional reactivation. In addition, we found that highly methylated areas of pericentromeres and chromosome arms are comparably affected by demethylating agents and that CHH methylation is proportionally more impacted than CG or CHG by AZA. This could be due to indirect effects, as CHH methyltransferases rely in part on CG and CHG methylation (Stroud et al. 2013). Alternatively, at high concentrations, AZA may have a greater initial effect that persists over cell division.

We find that when *A. thaliana* is treated with either AZA or ZEB, there is a comparable concentration-dependent loss of DNA methylation for all sequence contexts across gbM genes, mCHH genes, and transposons. RNA-seq data revealed that these chemicals have a disproportionate transcriptional impact on mCHH genes and transposons. The enrichment for mCHH, as opposed to mCHG, gene reactivation suggested that transcriptionally silenced genes contain high levels of all three contexts of methylation. Among TE genes, CACTA-like elements were the most highly upregulated. This category of mobile element is primarily localized in the pericentromeric region of chromosomes (Miura et al. 2004) and they have been found to be upregulated in *ddm1* mutants (Jeddeloh et al. 1999; Brzeski and Jerzmanowski 2003). Their low copy number and chromosomal position in *A. thaliana* hint that their expression is likely suppressed

due to the deleterious effects of their transposition (Miura et al. 2004). Further, although it has been shown that DNA methylation is largely recovered in adult plant tissue after treatment with methylation inhibitors (Baubec et al. 2009), the lasting effect of treatment may go beyond each plants epigenetic profile. After inhibitor treatment, if transposition occurs in the germline or somatic tissue cells that are germline-progenitors, then any TE-inflicted mutations would be passed to subsequent generations. WGBS experiments on the offspring of inhibitor-treated plants could help answer questions about increased TE gene transposition and the impact of new insertions on DNA methylation of surrounding DNA.

Although AZA has been shown to be less stable than ZEB (Pecinka and Liu 2014), it causes approximately the same magnitude of DNA methylation loss genome-wide after 10 days of seedling growth and appears to have a greater effect at high concentrations. This may be due to ZEB incorporating less frequently into the DNA double helix (Jones and Taylor 1980; Ben-Kasus et al. 2005; Liu et al. 2015) or binding less strongly to DNA methyltransferases (Champion et al. 2010). Indeed, a recent assay of ZEB-treated *A. thaliana* did not detect deoxyzebularine (the processed, deoxyribonucleotide version of ZEB) in DNA at a sensitivity of ~1 deoxyzebularine to 5000 deoxycytidine, showing that it does not incorporate into DNA efficiently (Liu et al. 2015). Furthermore, the primary DNA repair pathways that are activated in ZEB- and AZA-treated plants were shown to differ. Nucleotide excision is the dominant pathway in the of repair AZA-induced DNA damage, while homologous recombination was found to mainly mediate ZEB-induced damage repair (Liu et al. 2015). Any difference in the rate at which these nucleotide analogs are removed from the DNA helix may contribute to a difference in the amount of inhibitor-caused demethylation.

Here we demonstrate that AZA and ZEB treatment of *A. thaliana* results in similar changes in DNA methylation across the genome. In some ways, this is unexpected, given the evidence they may incorporate into DNA differently and largely be repaired by different pathways. Although some difference in the magnitude of DNA methylation loss may exist between AZA- or ZEB-treated plants, the biological impact of the disparity is not yet known. Having used aggregated WGBS data from a population of cells, there is no easy way of knowing the effect on specific individual cells. Furthermore, experimental comparison is needed to determine if such a difference is impactful or whether the difference is biologically negligible. This study provides a detailed look into the genome-wide and transcriptional effects of commonly used DNA methylation inhibitors.

Acknowledgements

We would like to thank Ortrun Mittelsten Scheid for critical comments and suggestions on this study. This work was supported by the National Science Foundation (NSF) (MCB – 1402183), by the Office of the Vice President of Research at UGA, and by The Pew Charitable Trusts to R.J.S. C.E.N was supported by a NSF postdoctoral fellowship (IOS – 1402183).

Work Cited

- Baubec T, Finke A, Mittelsten Scheid O, Pecinka A. 2014. Meristem-specific expression of epigenetic regulators safeguards transposon silencing in Arabidopsis. *EMBO reports* **15**: 446-452.
- Baubec T, Pecinka A, Rozhon W, Mittelsten Scheid O. 2009. Effective, homogeneous and transient interference with cytosine methylation in plant genomic DNA by zebularine. *The Plant journal : for cell and molecular biology* **57**: 542-554.
- Ben-Kasus T, Ben-Zvi Z, Marquez VE, Kelley JA, Agbaria R. 2005. Metabolic activation of zebularine, a novel DNA methylation inhibitor, in human bladder carcinoma cells. *Biochemical pharmacology* **70**: 121-133.
- Bewick AJ, Hofmeister BT, Lee K, Zhang X, Hall DW, Schmitz RJ. 2015. FASTmC: A Suite of Predictive Models for Nonreference-Based Estimations of DNA Methylation. *G3 (Bethesda, Md)* **6**: 447-452.
- Bewick AJ, Ji L, Niederhuth CE, Willing E-M, Hofmeister BT, Shi X, Wang L, Lu Z, Rohr NA, Hartwig B et al. 2016. On the Origin and Evolutionary Consequences of Gene Body DNA Methylation. *bioRxiv* doi:10.1101/045542.
- Brzeski J, Jerzmanowski A. 2003. Deficient in DNA methylation 1 (DDM1) defines a novel family of chromatin-remodeling factors. *The Journal of biological chemistry* **278**: 823-828.
- Cao X, Aufsatz W, Zilberman D, Mette MF, Huang MS, Matzke M, Jacobsen SE. 2003. Role of the DRM and CMT3 methyltransferases in RNA-directed DNA methylation. *Current biology : CB* **13**: 2212-2217.
- Champion C, Guianvarc'h D, Senamaud-Beaufort C, Jurkowska RZ, Jeltsch A, Ponger L, Arimondo PB, Guieysse-Peugeot AL. 2010. Mechanistic insights on the inhibition of c5 DNA methyltransferases by zebularine. *PloS one* **5**: e12388.
- Chang S, Pikaard CS. 2005. Transcript profiling in Arabidopsis reveals complex responses to global inhibition of DNA methylation and histone deacetylation. *The Journal of biological chemistry* **280**: 796-804.
- Christman JK, Mendelsohn N, Herzog D, Schneiderman N. 1983. Effect of 5-azacytidine on differentiation and DNA methylation in human promyelocytic leukemia cells (HL-60). *Cancer research* **43**: 763-769.
- Cokus SJ, Feng S, Zhang X, Chen Z, Merriman B, Haudenschild CD, Pradhan S, Nelson SF, Pellegrini M, Jacobsen SE. 2008. Shotgun bisulphite sequencing of the Arabidopsis genome reveals DNA methylation patterning. *Nature* **452**: 215-219.
- Creusot F, Acs G, Christman JK. 1982. Inhibition of DNA methyltransferase and induction of Friend erythroleukemia cell differentiation by 5-azacytidine and 5-aza-2'-deoxycytidine. *The Journal of biological chemistry* **257**: 2041-2048.
- Dieguez MJ, Bellotto M, Afsar K, Mittelsten Scheid O, Paszkowski J. 1997. Methylation of cytosines in nonconventional methylation acceptor sites can contribute to reduced gene expression. *Molecular & general genetics : MGG* **253**: 581-588.
- Du J, Zhong X, Bernatavichute YV, Stroud H, Feng S, Caro E, Vashisht AA, Terragni J, Chin HG, Tu A et al. 2012. Dual binding of chromomethylase domains to H3K9me2-containing nucleosomes directs DNA methylation in plants. *Cell* **151**: 167-180.

- Finnegan EJ, Brettell RI, Dennis ES. 1993. The role of DNA methylation in the regulation of plant gene expression. *Exs* **64**: 218-261.
- Finnegan EJ, Peacock WJ, Dennis ES. 1996. Reduced DNA methylation in *Arabidopsis thaliana* results in abnormal plant development. *Proceedings of the National Academy of Sciences of the United States of America* **93**: 8449-8454.
- Gal-Yam EN, Egger G, Iniguez L, Holster H, Einarsson S, Zhang X, Lin JC, Liang G, Jones PA, Tanay A. 2008. Frequent switching of Polycomb repressive marks and DNA hypermethylation in the PC3 prostate cancer cell line. *Proceedings of the National Academy of Sciences of the United States of America* **105**: 12979-12984.
- Henderson IR, Jacobsen SE. 2008. Tandem repeats upstream of the *Arabidopsis* endogene SDC recruit non-CG DNA methylation and initiate siRNA spreading. *Genes & development* **22**: 1597-1606.
- Hohn T, Corsten S, Rieke S, Muller M, Rothnie H. 1996. Methylation of coding region alone inhibits gene expression in plant protoplasts. *Proceedings of the National Academy of Sciences of the United States of America* **93**: 8334-8339.
- Jackson JP, Lindroth AM, Cao X, Jacobsen SE. 2002. Control of CpNpG DNA methylation by the KRYPTONITE histone H3 methyltransferase. *Nature* **416**: 556-560.
- Jeddeloh JA, Stokes TL, Richards EJ. 1999. Maintenance of genomic methylation requires a SWI2/SNF2-like protein. *Nature genetics* **22**: 94-97.
- Ji L, Neumann DA, Schmitz RJ. 2015. Crop Epigenomics: Identifying, Unlocking, and Harnessing Cryptic Variation in Crop Genomes. *Molecular plant* **8**: 860-870.
- Johannes F, Porcher E, Teixeira FK, Saliba-Colombani V, Simon M, Agier N, Bulski A, Albuissou J, Heredia F, Audigier P et al. 2009. Assessing the impact of transgenerational epigenetic variation on complex traits. *PLoS genetics* **5**: e1000530.
- Jones PA, Taylor SM. 1980. Cellular differentiation, cytidine analogs and DNA methylation. *Cell* **20**: 85-93.
- Kafri T, Ariel M, Brandeis M, Shemer R, Urven L, McCarrey J, Cedar H, Razin A. 1992. Developmental pattern of gene-specific DNA methylation in the mouse embryo and germ line. *Genes & development* **6**: 705-714.
- Kim D, Pertea G, Trapnell C, Pimentel H, Kelley R, Salzberg SL. 2013. TopHat2: accurate alignment of transcriptomes in the presence of insertions, deletions and gene fusions. *Genome biology* **14**: R36.
- Kinoshita Y, Saze H, Kinoshita T, Miura A, Soppe WJ, Koornneef M, Kakutani T. 2007. Control of FWA gene silencing in *Arabidopsis thaliana* by SINE-related direct repeats. *The Plant journal : for cell and molecular biology* **49**: 38-45.
- Law JA, Jacobsen SE. 2010. Establishing, maintaining and modifying DNA methylation patterns in plants and animals. *Nature reviews Genetics* **11**: 204-220.
- Lister R, O'Malley RC, Tonti-Filippini J, Gregory BD, Berry CC, Millar AH, Ecker JR. 2008. Highly integrated single-base resolution maps of the epigenome in *Arabidopsis*. *Cell* **133**: 523-536.
- Liu CH, Finke A, Diaz M, Rozhon W, Poppenberger B, Baubec T, Pecinka A. 2015. Repair of DNA Damage Induced by the Cytidine Analog Zebularine Requires ATR and ATM in *Arabidopsis*. *The Plant cell* **27**: 1788-1800.

- Mathieu O, Reinders J, Caikovski M, Smathajitt C, Paszkowski J. 2007. Transgenerational stability of the Arabidopsis epigenome is coordinated by CG methylation. *Cell* **130**: 851-862.
- Miura A, Kato M, Watanabe K, Kawabe A, Kotani H, Kakutani T. 2004. Genomic localization of endogenous mobile CACTA family transposons in natural variants of Arabidopsis thaliana. *Molecular genetics and genomics : MGG* **270**: 524-532.
- Niederhuth CE, Bewick AJ, Ji L, Alabady M, Kim KD, Li Q, Rohr NA, Rambani A, Burke JM, Udall JA et al. 2016. Widespread natural variation of DNA methylation within angiosperms. *bioRxiv* doi:10.1101/045880.
- Niederhuth CE, Schmitz RJ. 2014. Covering your bases: inheritance of DNA methylation in plant genomes. *Molecular plant* **7**: 472-480.
- Ohm JE, McGarvey KM, Yu X, Cheng L, Schuebel KE, Cope L, Mohammad HP, Chen W, Daniel VC, Yu W et al. 2007. A stem cell-like chromatin pattern may predispose tumor suppressor genes to DNA hypermethylation and heritable silencing. *Nature genetics* **39**: 237-242.
- Pecinka A, Liu CH. 2014. Drugs for plant chromosome and chromatin research. *Cytogenetic and genome research* **143**: 51-59.
- Quinlan AR, Hall IM. 2010. BEDTools: a flexible suite of utilities for comparing genomic features. *Bioinformatics (Oxford, England)* **26**: 841-842.
- Reinders J, Wulff BB, Mirouze M, Mari-Ordonez A, Dapp M, Rozhon W, Bucher E, Theiler G, Paszkowski J. 2009. Compromised stability of DNA methylation and transposon immobilization in mosaic Arabidopsis epigenomes. *Genes & development* **23**: 939-950.
- Santi DV, Norment A, Garrett CE. 1984. Covalent bond formation between a DNA-cytosine methyltransferase and DNA containing 5-azacytosine. *Proceedings of the National Academy of Sciences of the United States of America* **81**: 6993-6997.
- Saze H, Kakutani T. 2007. Heritable epigenetic mutation of a transposon-flanked Arabidopsis gene due to lack of the chromatin-remodeling factor DDM1. *The EMBO journal* **26**: 3641-3652.
- Schultz MD, He Y, Whitaker JW, Hariharan M, Mukamel EA, Leung D, Rajagopal N, Nery JR, Urich MA, Chen H et al. 2015a. Human body epigenome maps reveal noncanonical DNA methylation variation. *Nature* **523**: 212-216.
- Schultz MD, He Y, Whitaker JW, Hariharan M, Mukamel EA, Leung D, Rajagopal N, Nery JR, Urich MA, Chen H et al. 2015b. Human body epigenome maps reveal noncanonical DNA methylation variation. *Nature* doi:10.1038/nature14465.
- Schultz MD, Schmitz RJ, Ecker JR. 2012. 'Leveling' the playing field for analyses of single-base resolution DNA methylomes. *Trends in genetics : TIG* **28**: 583-585.
- Soppe WJ, Jacobsen SE, Alonso-Blanco C, Jackson JP, Kakutani T, Koornneef M, Peeters AJ. 2000. The late flowering phenotype of fwa mutants is caused by gain-of-function epigenetic alleles of a homeodomain gene. *Molecular cell* **6**: 791-802.
- Stroud H, Greenberg MV, Feng S, Bernatavichute YV, Jacobsen SE. 2013. Comprehensive analysis of silencing mutants reveals complex regulation of the Arabidopsis methylome. *Cell* **152**: 352-364.
- Takuno S, Gaut BS. 2012. Body-methylated genes in Arabidopsis thaliana are functionally important and evolve slowly. *Molecular biology and evolution* **29**: 219-227.

- Tran RK, Henikoff JG, Zilberman D, Ditt RF, Jacobsen SE, Henikoff S. 2005. DNA methylation profiling identifies CG methylation clusters in Arabidopsis genes. *Current biology : CB* **15**: 154-159.
- Trapnell C, Hendrickson DG, Sauvageau M, Goff L, Rinn JL, Pachter L. 2013. Differential analysis of gene regulation at transcript resolution with RNA-seq. *Nature biotechnology* **31**: 46-53.
- Urich MA, Nery JR, Lister R, Schmitz RJ, Ecker JR. 2015. MethylC-seq library preparation for base-resolution whole-genome bisulfite sequencing. *Nature protocols* **10**: 475-483.
- Widschwendter M, Fiegl H, Egle D, Mueller-Holzner E, Spizzo G, Marth C, Weisenberger DJ, Campan M, Young J, Jacobs I et al. 2007. Epigenetic stem cell signature in cancer. *Nature genetics* **39**: 157-158.
- Zemach A, Kim MY, Hsieh PH, Coleman-Derr D, Eshed-Williams L, Thao K, Harmer SL, Zilberman D. 2013. The Arabidopsis nucleosome remodeler DDM1 allows DNA methyltransferases to access H1-containing heterochromatin. *Cell* **153**: 193-205.
- Zhang X, Yazaki J, Sundaresan A, Cokus S, Chan SW, Chen H, Henderson IR, Shinn P, Pellegrini M, Jacobsen SE et al. 2006. Genome-wide high-resolution mapping and functional analysis of DNA methylation in arabidopsis. *Cell* **126**: 1189-1201.
- Zilberman D, Gehring M, Tran RK, Ballinger T, Henikoff S. 2007. Genome-wide analysis of Arabidopsis thaliana DNA methylation uncovers an interdependence between methylation and transcription. *Nature genetics* **39**: 61-69.

Figure Legends

Figure 1 | AZA and ZEB treatment result in non-selective, concentration-dependent loss of DNA methylation genome-wide

- A. The genome-wide methylation level of the control seedlings (0 μ M) and seedlings treated with 25 μ M, 50 μ M, and 100 μ M of either AZA or ZEB.
- B. The methylation level of AZA- and ZEB-treated seedlings relative to the untreated control (treated/control) shown side-by-side for each context of DNA methylation. Both AZA and ZEB were compared to the untreated control methylation levels.
- C. A frequency distribution of the methylation levels of individual methylated cytosines for both AZA and ZEB treatments and the controls. In mock-treated samples, many methylated CG sites are 100% methylated, whereas in treated samples, most of the sites are not completely methylated.

Figure 2 | AZA and ZEB cause a concentration-dependent loss of DNA methylation across chromosome 1

- A. The methylation level (all contexts) for each discrete 50 Kb window across chromosome 1 shown for untreated control samples and each treatment concentration of both AZA and ZEB. The dashed lines partition 7.5 Mb of area

that was defined as the pericentromeric region of the chromosome. Refer to the legend for the concentration and context of methylation that each line represents. B. The methylation level of AZA-treated (left) and ZEB-treated (right) DNA relative to the mock-treated control is mapped across chromosome 1 for each 50 Kb region.

C-D. A pairwise comparison of methylation level in mock-treated control seedlings and 100 μ M AZA-treated seedlings for highly methylated 100 bp windows in both the pericentromere and the chromosome arms (as defined in 3A). CG (C) and CHH (D) contexts of DNA methylation are shown. A highly methylated window was defined as having $\geq 50\%$ methylation in the control sample for CG and $\geq 30\%$ methylation in the control sample for CHH. AZA-treated seedling methylation level is on the y-axis and control methylation level is on the x-axis. The color spectrum—ranging from red (low) to purple (high)— illustrates the density of points at a coordinate. The slopes (m) of the dashed lines represent the following relative methylation levels: 100% (treated and control methylation level are the same), 75%, 50% (treated methylation level is half of the control), and 25%.

Figure 3 | AZA and ZEB cause similar patterns of DNA methylation loss and increase expression of genes highly methylated in all contexts

A-C. The methylation level across all gene-body, CHH-enriched (mCHH), and TE genes are depicted for 100 μ M AZA (red), 100 μ M ZEB (blue), and untreated control (green).

D. A pie chart depicting the types of genes upregulated by AZA treatment (right) compared with all genes annotated by TAIR10 (left).

E-F. The percent of genes (protein-coding and TE) that are significantly upregulated when treated with 100 μ M of AZA is shown. Statistical enrichment based on a Fischer two-sided test is denoted by * for p value < 0.05 , ** < 0.01 , and *** < 0.001 .

Figure 4 | FWA and SDC methylation level decreases and mRNA expression increases in response to chemical demethylating agents

A-B. Browser screenshots of the methylation mapped to the *A. thaliana* genome show single base pair resolution data on individual cytosines for *SDC* and *FWA*. The legend box (outlined in red) shows that the height and the color of the bar illustrate the methylation level and context of each cytosine, whereas the direction of the bar indicates the strand. The genes themselves are mapped below the methylation data with the UTRs in blue, coding regions in yellow, and introns as the black line connecting them.

C-D. The total methylation level (left) of the 5'UTR and upstream promoter region of genes *SDC* and *FWA* are depicted (U=Untreated, M=Mock). The black box in the browser screenshots surrounds the region analyzed for each gene.

Figure S1 | DNA methylation across all chromosomes is decreased when treated with AZA and ZEB in a concentration-dependent fashion

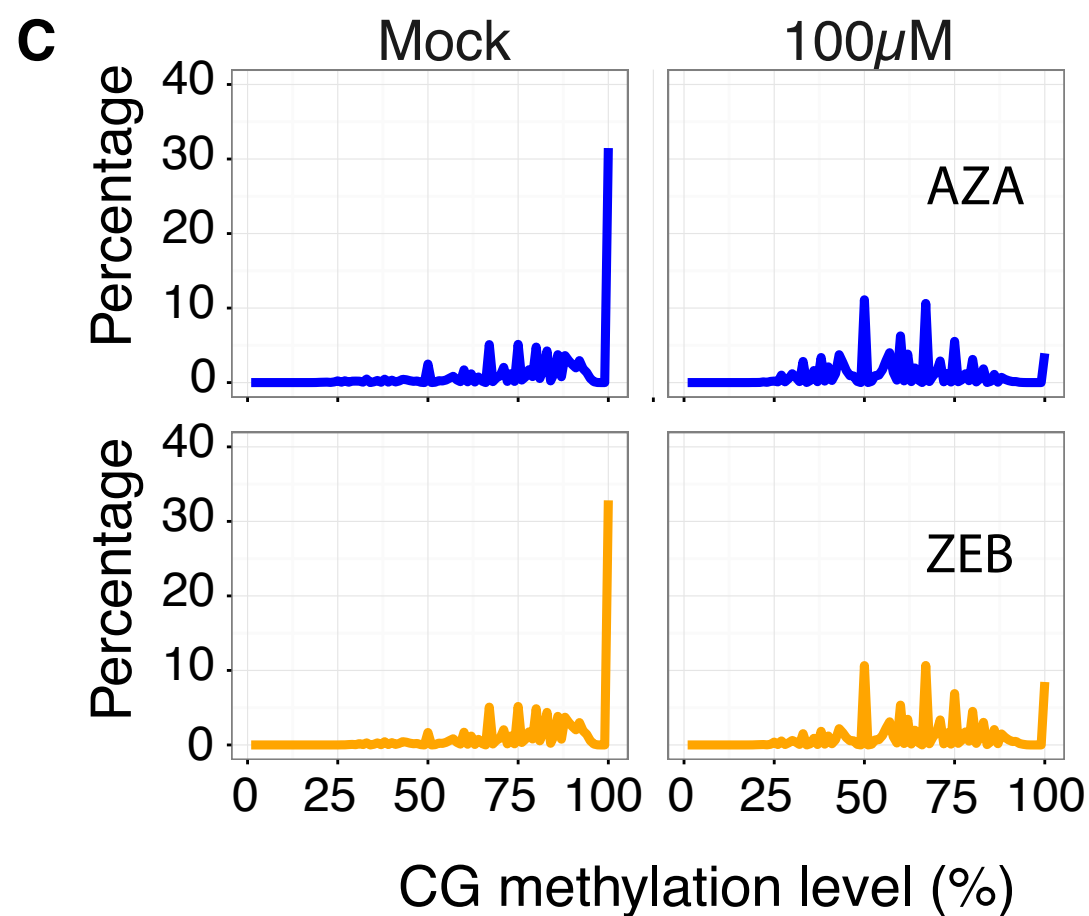
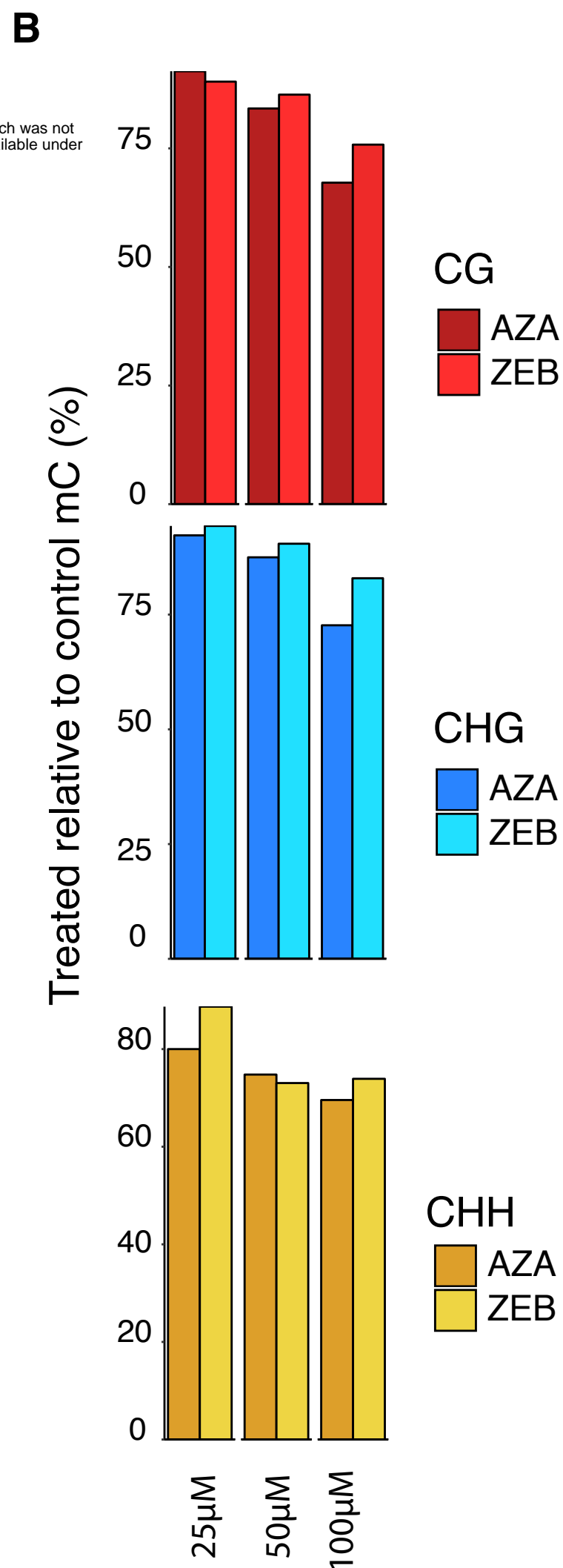
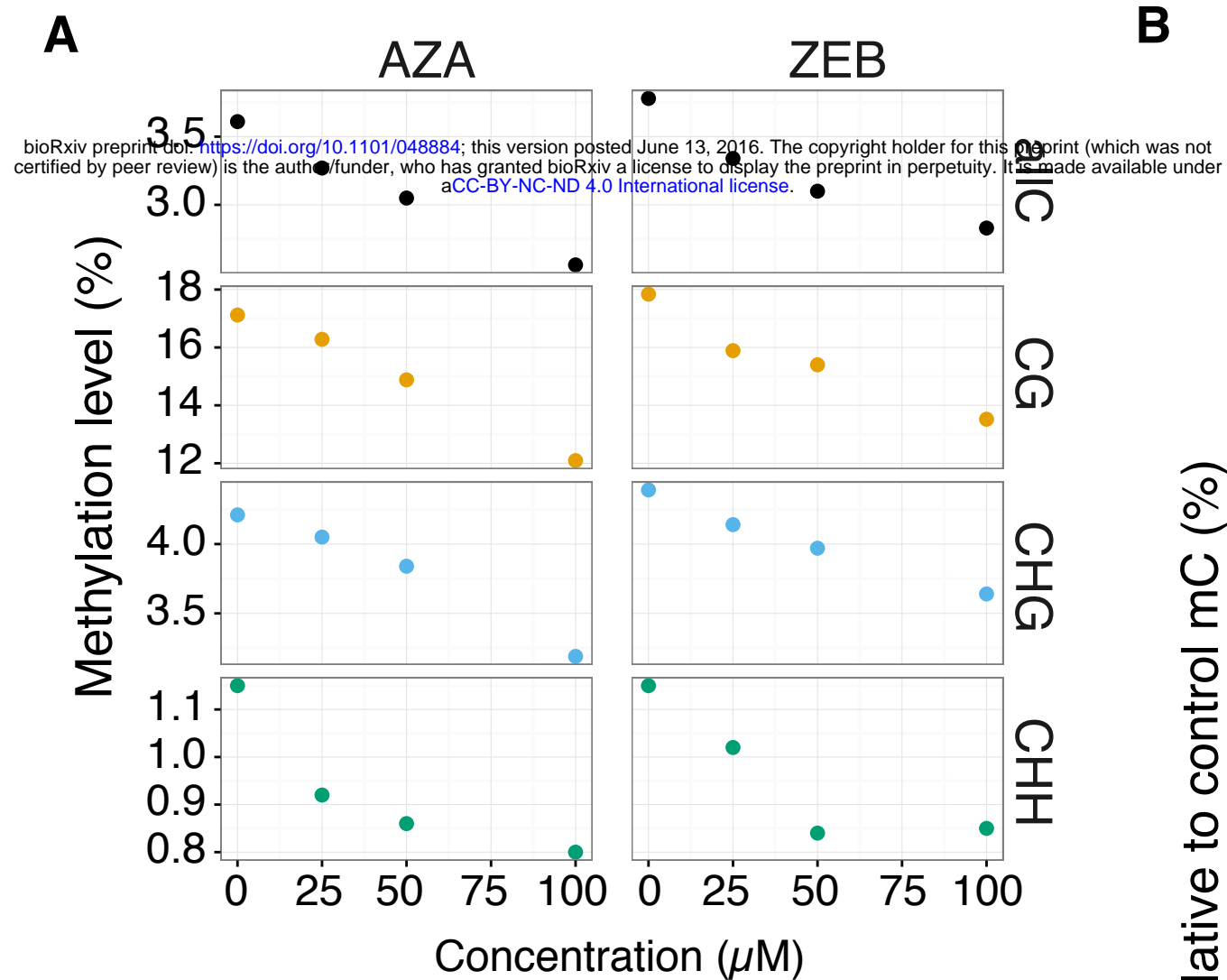
A-B. Relative methylation level shown across chromosomes 2-4 (chromosome 1 shown in Figure 2B) for AZA-treated (S1A) and ZEB-treated (S1B) seedlings.

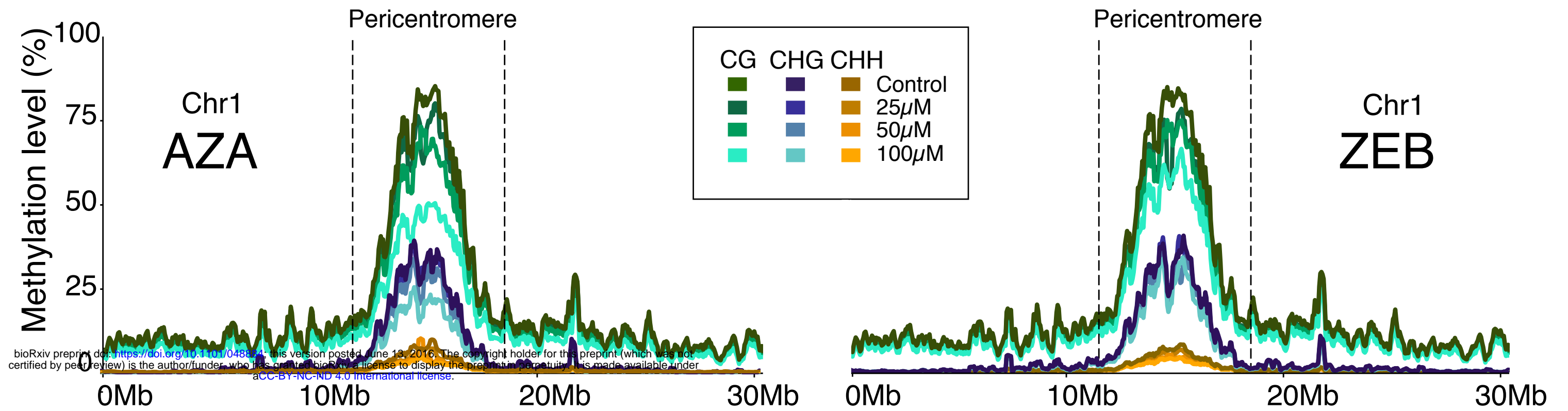
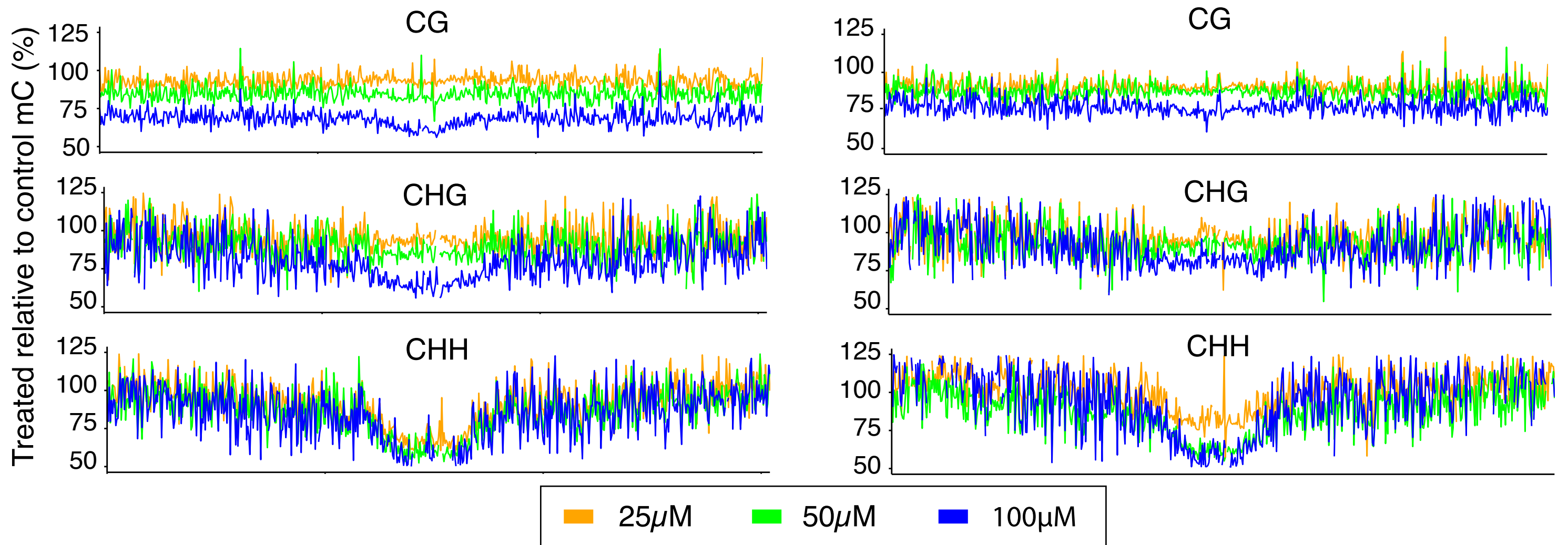
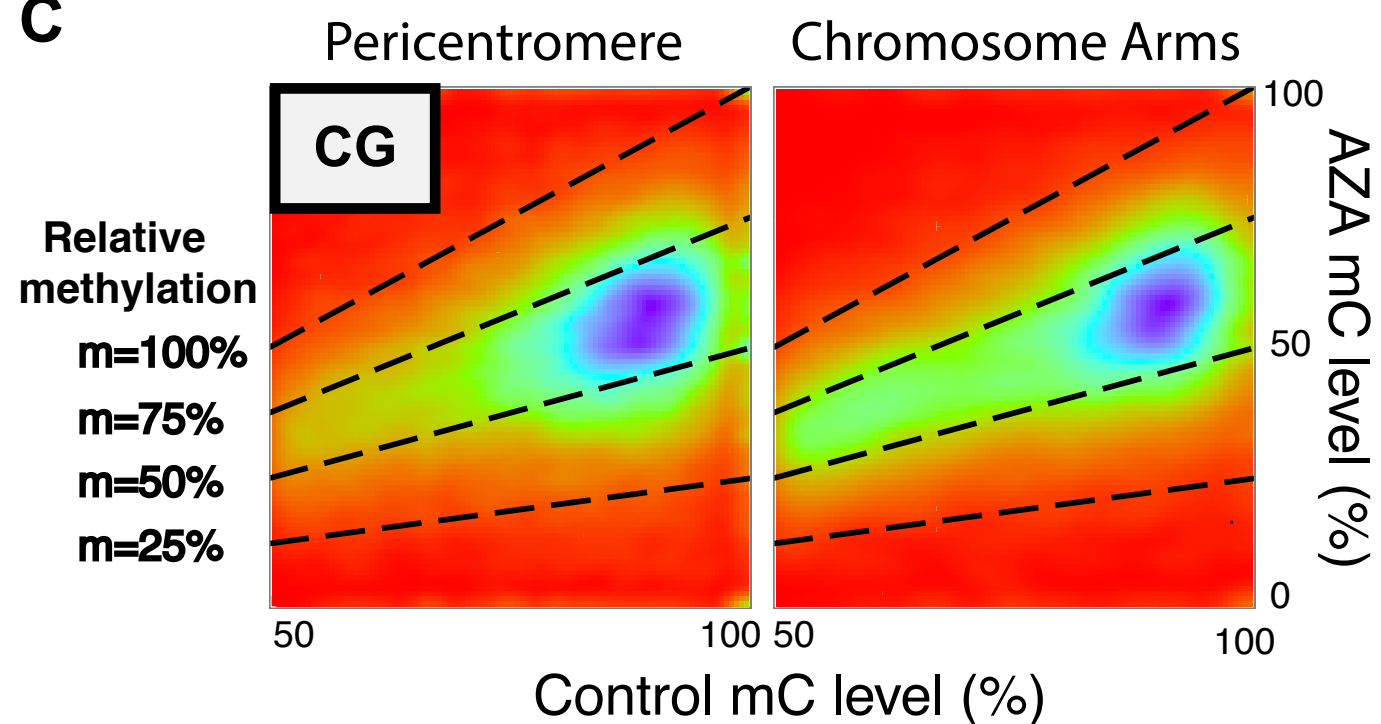
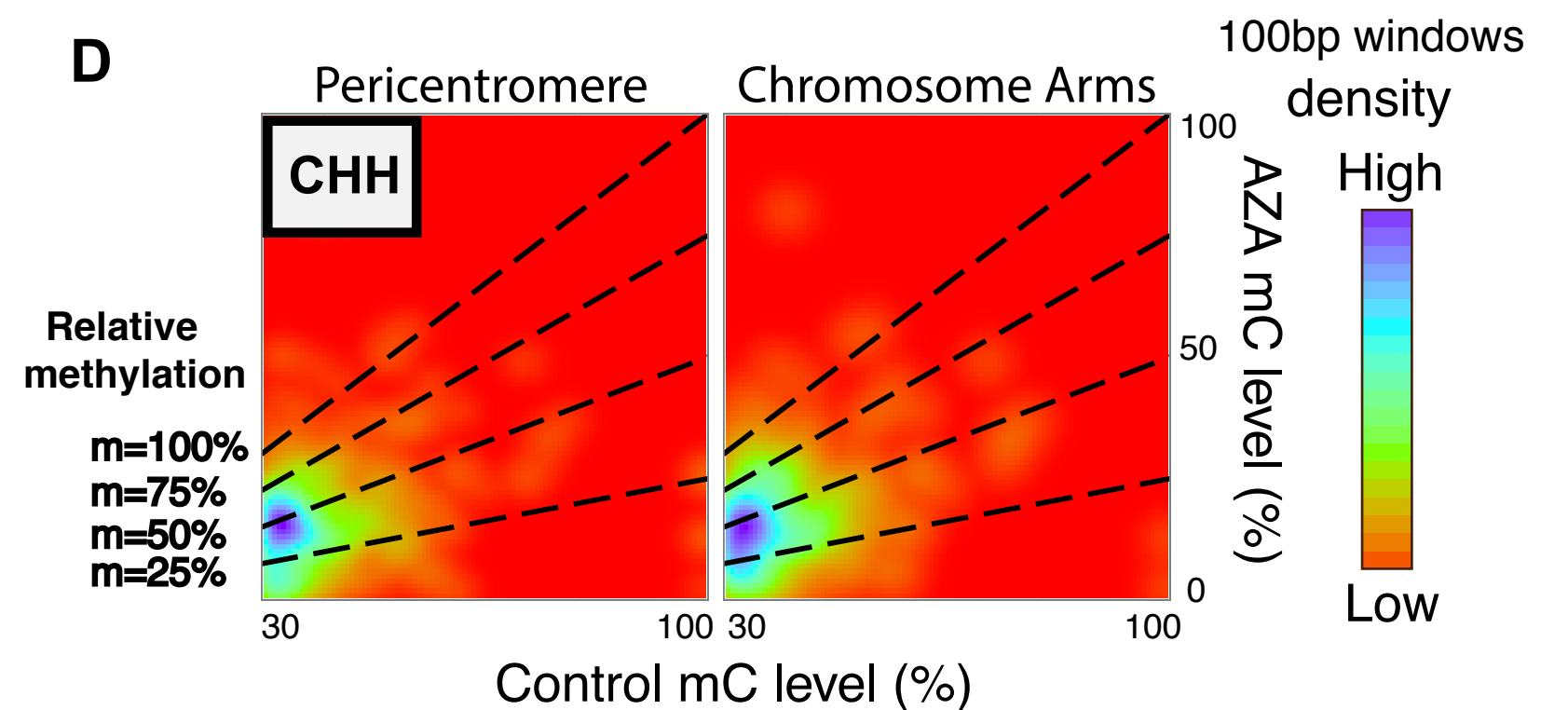
Figure S2 | AZA and ZEB induce a concentration-dependent decrease in DNA methylation in all types of genetic elements

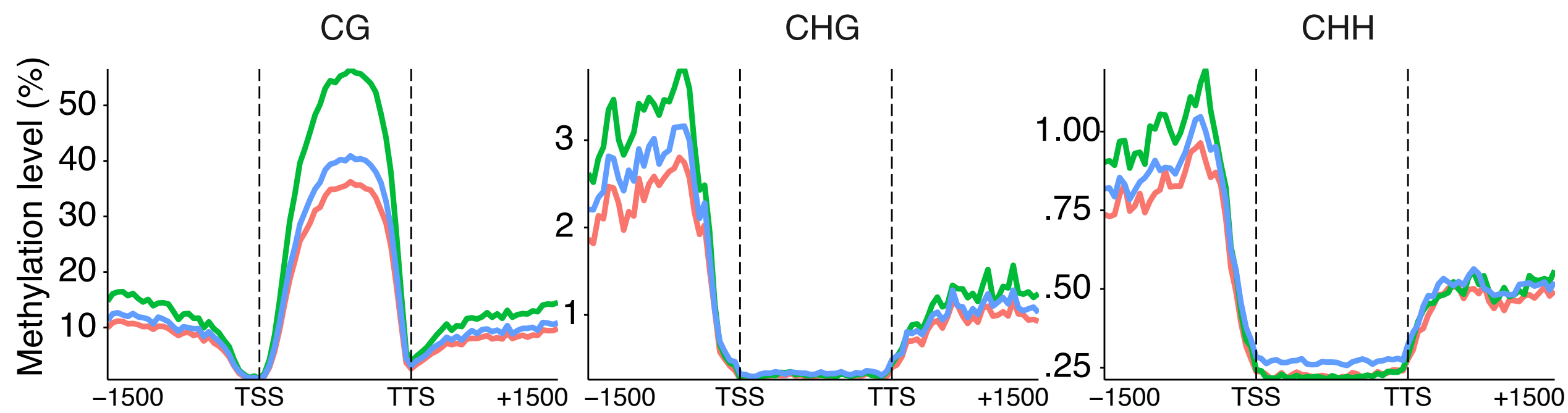
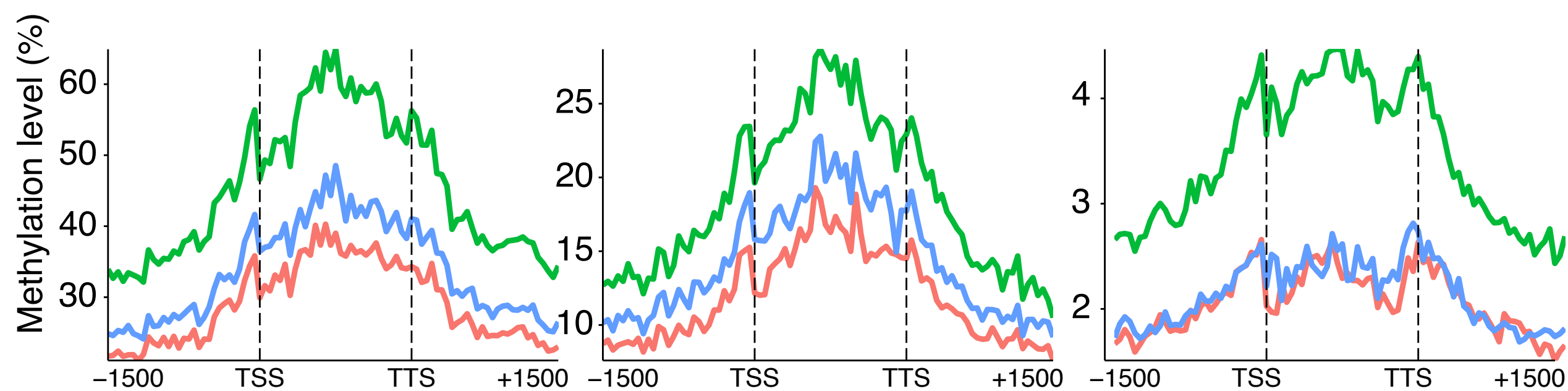
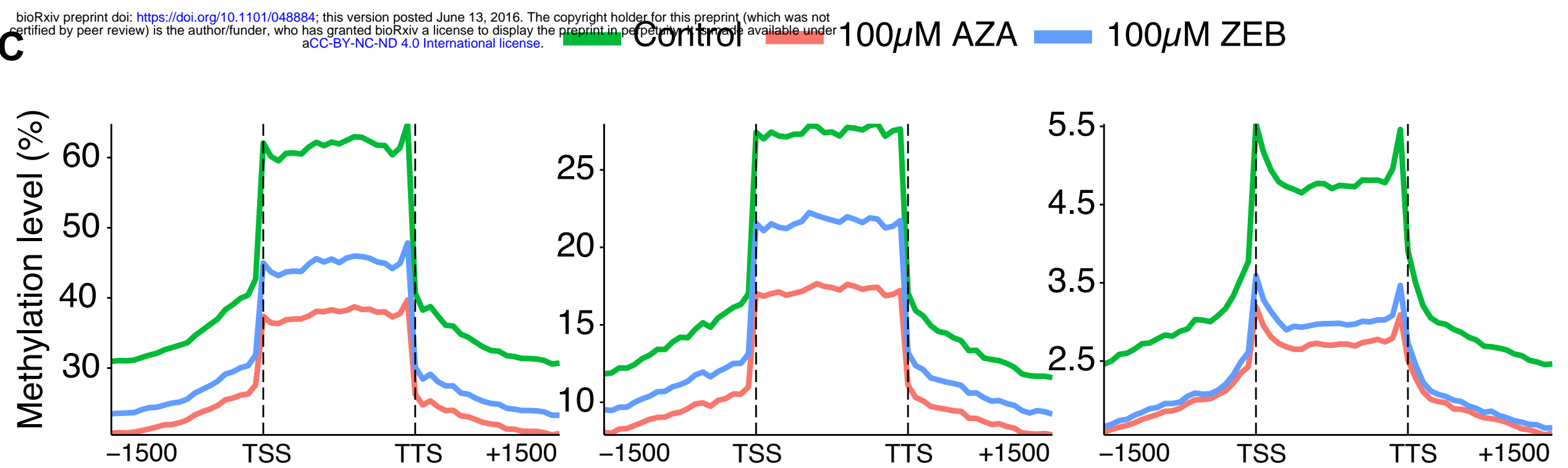
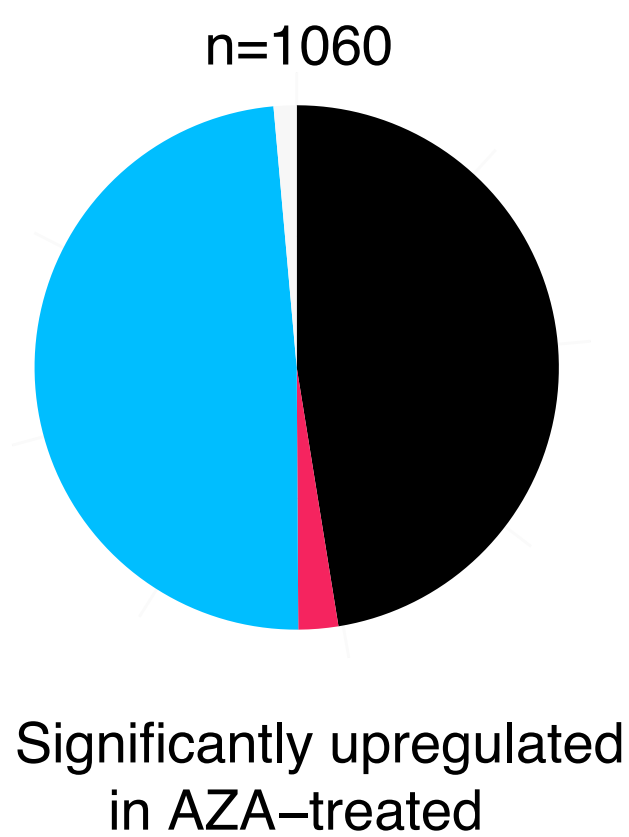
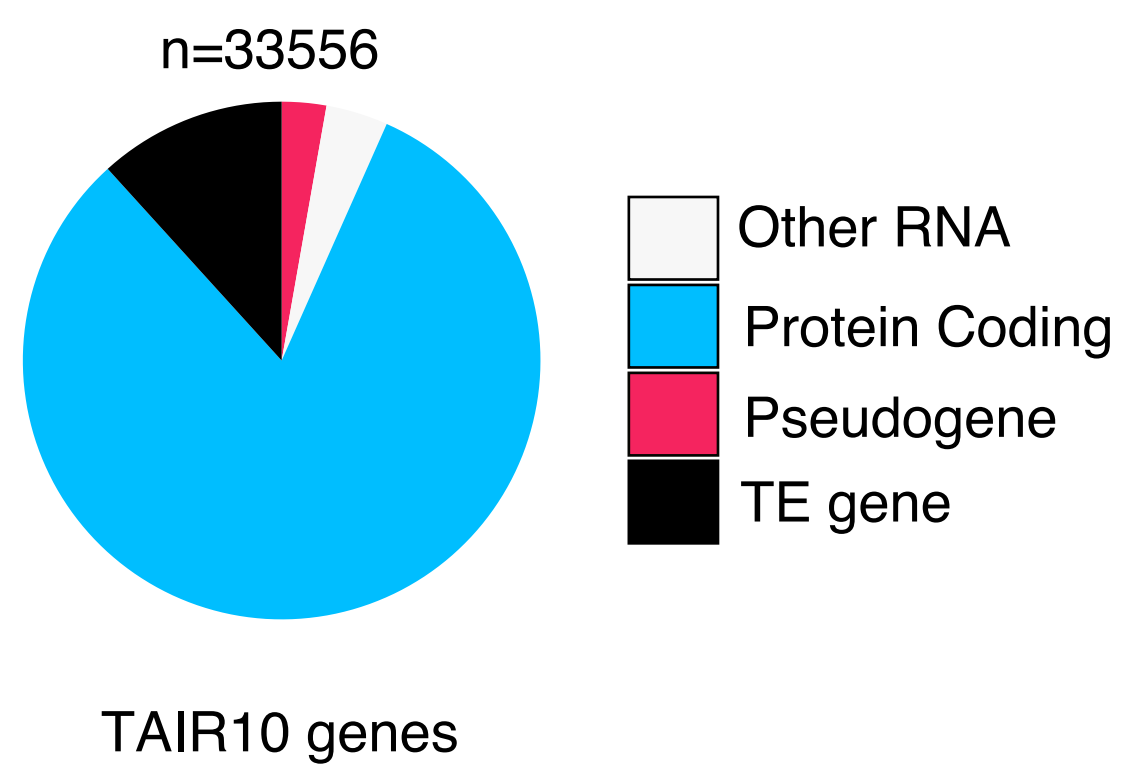
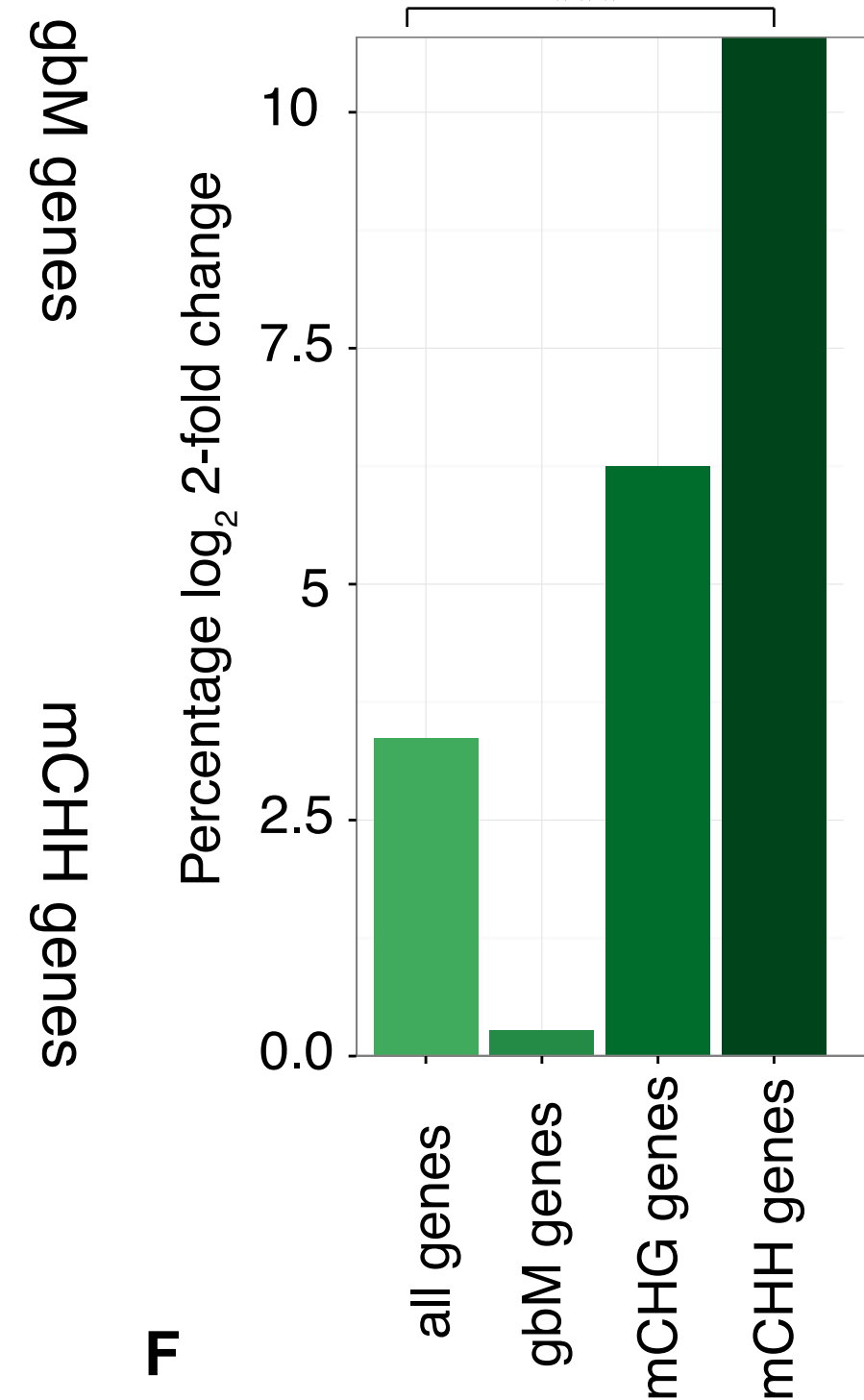
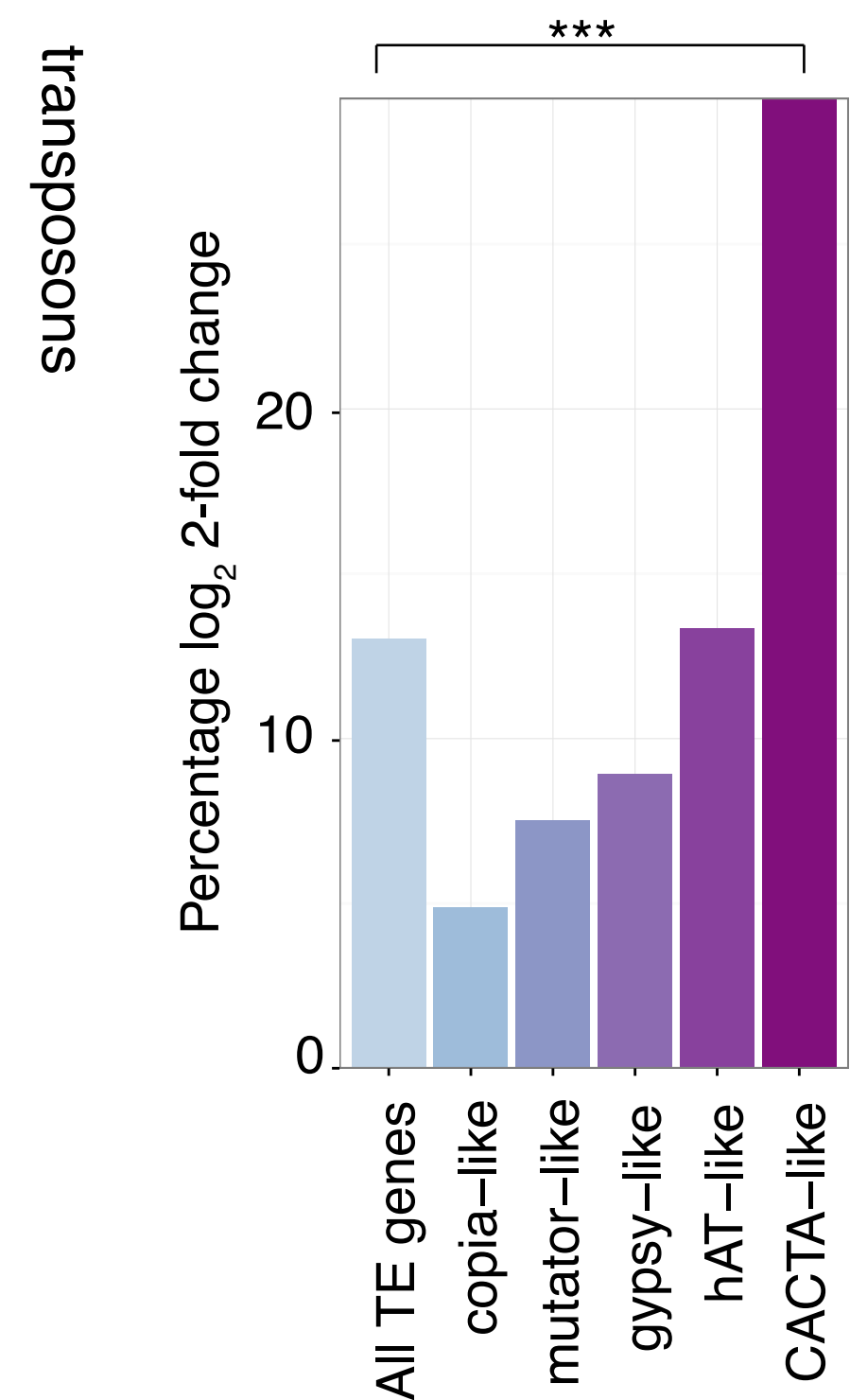
A-D. DNA methylation maps across four different categories of methylated genetic elements: gbM genes (A), CHG-enriched (mCHG) genes (B), CHH-enriched (mCHH) genes (C), transposons (D). The colors (top) represent the different treatment concentrations. The demethylating agent and sequence context is given above each vertical column of graphs.

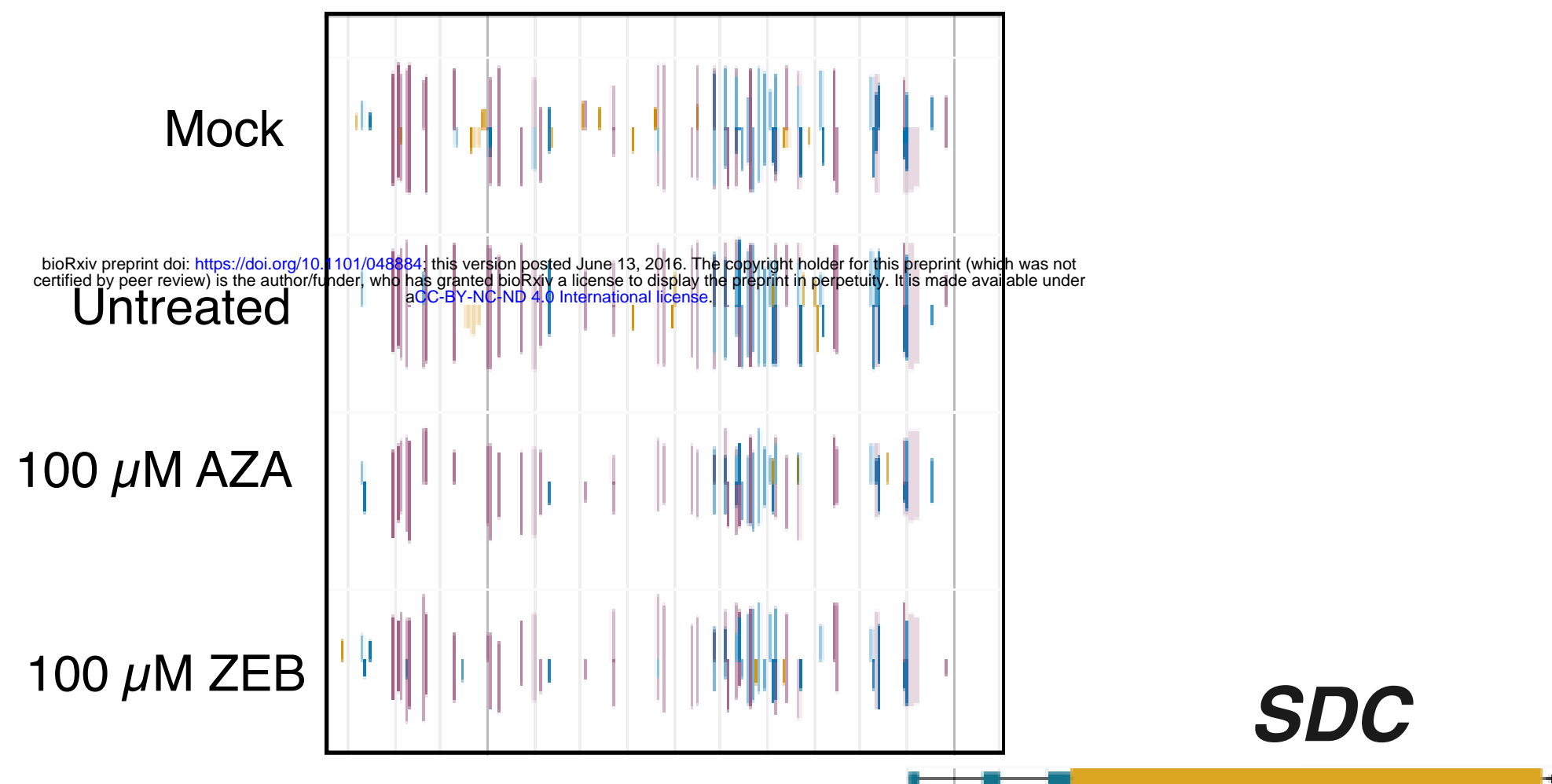
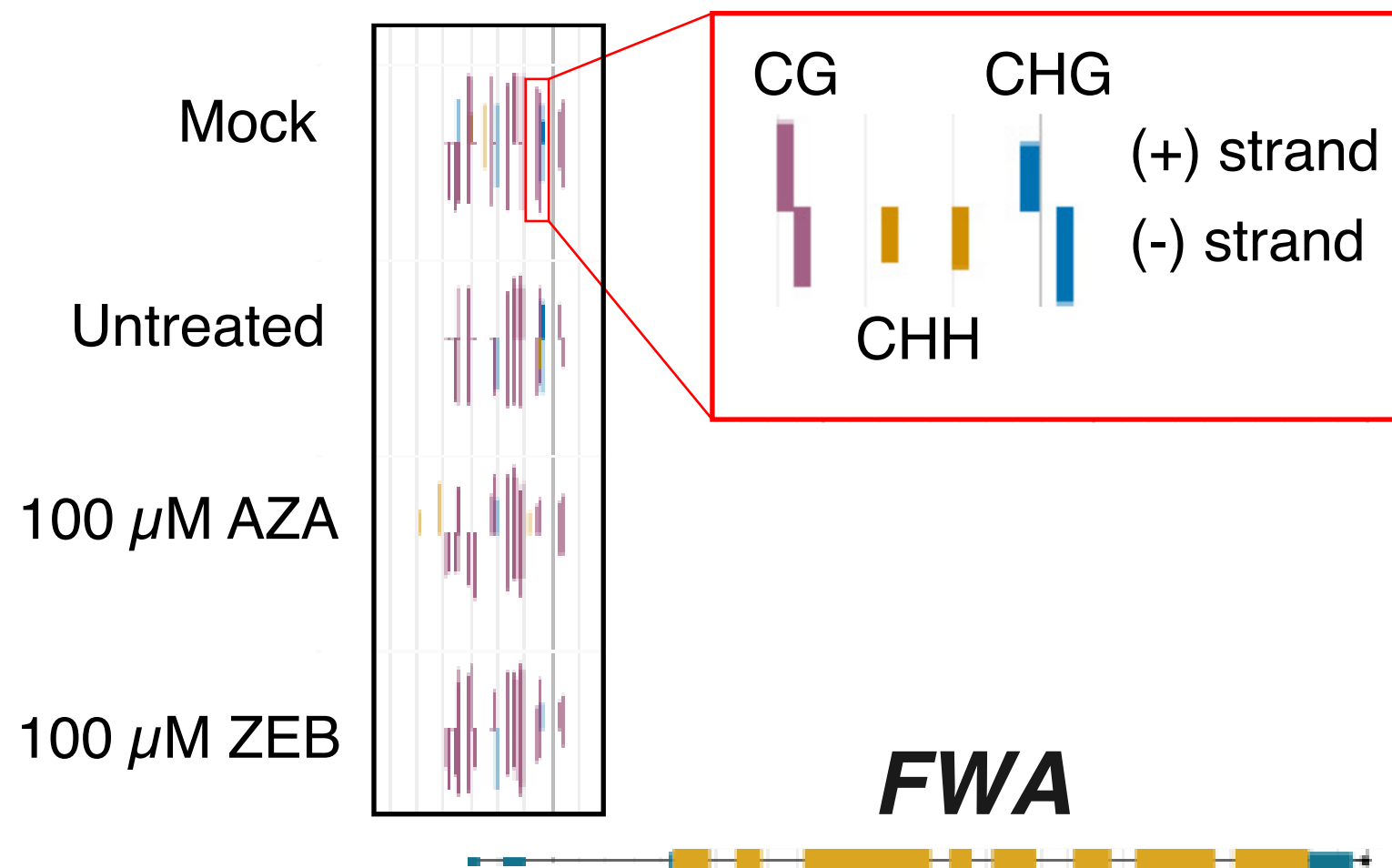
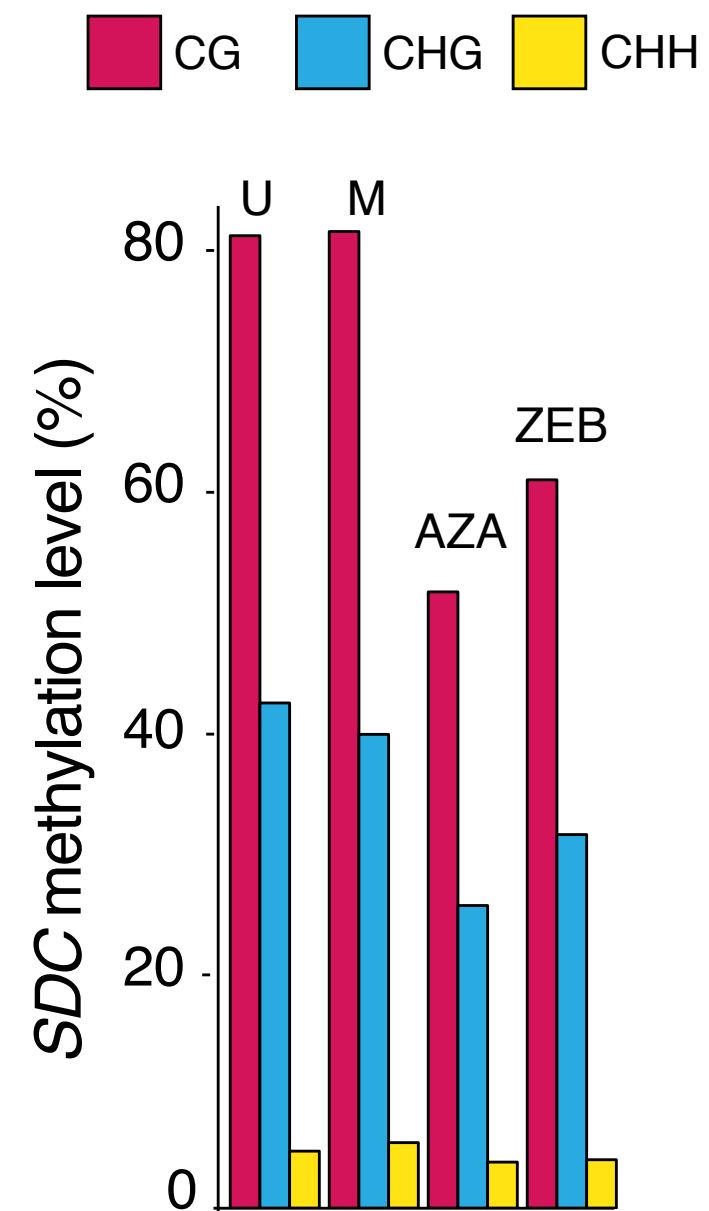
Figure S3 | Pairwise comparison of highly methylated 100 bp windows between ZEB-treated and control seedlings

A pairwise comparison of methylation level in untreated seedlings and the 100 μ M ZEB-treated seedlings for highly methylated 100 bp windows in both the pericentromere and the chromosome arms (as defined in Figure 2A). CG and CHH contexts of DNA methylation are shown. A highly methylated window was defined as having $\geq 50\%$ methylation in the control sample for CG and $\geq 30\%$ methylation in the control sample for CHH. ZEB-treated seedling methylation level is on the y-axis and control methylation level is on the x-axis. The color spectrum—ranging from red (low) to purple (high)— illustrates the density of points at a coordinate. The slopes (m) of the dashed lines represent the following relative methylation levels: 100% (treated and control methylation level are the same), 75%, 50% (treated methylation level is half of the control), and 25%.



A**B****C****D**

A**B****C****D****E****F**

A**B****C****D**